Journal of the Korean Electrochemical Society
Vol. 9, No. 4, 2006, 151-157

CFD Simulation Tool for Anode-Supported Flat-Tube Solid Oxide Fuel Cell

M. Elsayed. Youssef, Tak-Hyoung Lim†, Rak-Hyun Song†, Seung-Bok Lee†, and Dong-Ryul Shin†

Mubarak City for Scientific Research and Technology Application, Informatic Institute, Egypt
†Korea Institute of Energy Research (KIER), P.O.Box 103, Yusong, Daejon 305-343, Korea

(Received October 12, 2006 : Accepted October 26, 2006)

Abstract : A two-dimensional numerical model to study the performance of anode-supported flat-tube solid oxide fuel cell (SOFC) for the cross section of the cell in the flow direction of the fuel and air flows is developed. In this model a mass and charge balance, Maxwell-Stefan equation as well as the momentum equation by using, Darcy's law are applied in differential form. The finite element method using FEMLAB commercial software is used for meshing, discritization and solving the system of coupled differential equations. The current density distribution and fuel consumption as well as water production are analyzed. Experimental data is used to verify a predicted voltage-current density and power density versus current density to judge on the model accuracy.

Key words : SOFC, Modeling, Simulation, FEMLAB, Chemical engineering module.

1. Introduction

A single tubular SOFC is viewed as a two-dimensional axial-symmetric one is studied by Pei-Wen Li *et al.*[1] In this research model is assumed that the heat and mass species do not exchange in between one cell and its neighboring cells. A most important result obtained by this model, that the two ends of fuel cell have a relatively low temperature, while the hotspot locates closer to the closed end of the cell tube when the operating current density is low with increasing current density, the hotspot shifts to the open-end side of the cell. A three-dimensional numerical model to simulate the heat/mass transfer and fluid flow of flat-tube high power density (HPD)-SOFC is developed by Yi Xin LU, *et al.*[2] In part II of this study which was carried out by Yi Xin LU and LauraSchefer[3] they studied the cell performance and stack optimization. The effects of the stack chamber number, stack shapes, and other stack geometry features on the performance of the flat-tube HPD SOFC were investigated. The main important results were obtained are the performance of a flat-tube HPD SOFC is better than a tubular SOFC with the same active cell surface, and the increasing the number of chambers number can improve the overall performance of a flat-tube HPD SOFC. J.R. Ferguson *et al*[4] presented a three-dimensional mathematical model of a solid oxide fuel cell. The mathematical model which was developed is based on a local balance approach, and the finite volume method. In this work different SOFC geometries, such as planar, tubular, and cylindrical ones were compared and cross-counter- and co-flow designs for a planar cell geometry was found that the counter-flow was optimal (for using hydrogen as a cell fuel). David J. Hall and R. Gerald Colclaser[5] developed a computer model for simulating the transient operation of a tubular solid oxide fuel cell. The model included the electrochemical, thermal and mass flow elements that effect SOFC electrical output. Roberto Bove *et al*[6] presented a review of the most significant SOFC models and then the possibility of their use in a macro-model is evaluated. They concluded that different results can be generated according to the assumptions made when adapting micro-model equations to a macro-model. A quantitative analysis of the differences between macro-and micro-model was performed and the reliability of the model was estimated. In the present work a two-dimensional model is developed to study the performance of SOFC anode supported tube. Mass balance, by using Maxwell-Stefan equation is used for gas mixture, hydrogen and water in anode and oxygen and nitrogen in a cathode. Momentum equation, Darcy's law is used to study the flow in porous media. Ionic and electronic current balance by using conductive media DC equation has been done.

*E-mail: drshin@kier.re.kr

2. Model Description

The governing equations which will be used to study mass transport and electrochemical reaction in SOFC are as follows:

1. Mass balance, Maxwell-Stefan equation will be used at the two electrodes, cathode and anode
2. Momentum equation, Darcy's law applied to study the flow in porous media, cathode and anode
3. Ionic current balance in electrolyte by using conductive media DC equation
4. Electronic current balance in cathode and anode by using conductive media DC equation

Fig. 1 shows the cross section of unit cell used in this

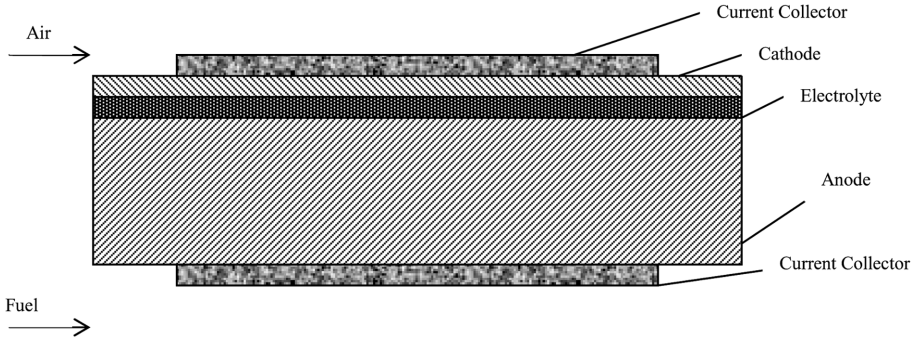

Fig. 1. Cross section of a unit cell.

study (not to scale)

The mass balance at steady state in the macroscopic structure is according to the following equation:

$$\nabla N_i = R_i \tag{1}$$

For species $i = N_2$, O_2 in the cathode and,
$i = H_2$, H_2O in the anode.

Where N_i denotes the flux vector and R_i denotes the consumption term. For nitrogen (N_2), the consumption term R_i is equal to zero. The flux vector is given by Fickean formulation, obtained from Maxwell-Stefan equations, so that the following equation for mass balance was obtained:

$$\nabla\left[-\rho\omega_i\sum_{j=1}^{n} D_{ij}\frac{M}{M_j}\left(\nabla\omega_j + \omega_j\frac{\nabla M}{M}\right)\right] = R_i \text{ in the two electrodes} \tag{2}$$

Where ρ denotes the density of the gas in cathode (air), and in anode (0.97 H_2 and 0.03 H_2O), ω_i is the mass fraction for species i, D_{ij} is the effective Maxwell-Stefan diffusivities (m^2 s^{-1}), M_j is the molar mass for species j (kg $mole^{-1}$), and M is the total molar for the gas mixture.

The density of the oxidizer (air) in the cathode can be calculated as follows:

$$\rho_{cat} = \frac{P_{atm}}{R_g T(0.21M_{O_2} + 0.79M_{N_2})} \tag{3}$$

$$\rho_{an} = \frac{P_{atm}}{R_g T(0.97M_{H_2} + 0.03M_{H_2O})} \tag{4}$$

Where P_{atm} denotes the atmospheric pressure (Pa)

The Maxwell-Stefan diffusivities can be described for cathode and anode with an empirical equation as showed by Wesselingh,[7] based on kinetic gas theory as follows:

$$D_{i-j} = K_D\frac{T^{1.75}}{P_{atm}(V_i^{1/3} + V_j^{1/3})}\left[\frac{1}{M_i} + \frac{1}{M_j}\right]^{1/2} \tag{5}$$

For the gas mixture in the cathode i denotes to oxygen and j for nitrogen while the gas mixture in the anode i is used for hydrogen and j for water.

Where K_D is constant, V_i denotes the molar diffusion volume of species i (m^3 $mole^{-1}$)

The molar diffusion volume (V_i) for simple molecules are used as by Perry.[8]

In the porous cathode and anode, the effective binary diffusivities depend on the porosity (ε), of the two electrodes according to:

$$D_{i-j}^{eff} = D_{i-j}\varepsilon^{1.5} \tag{6}$$

The balance of the current induced by the migration of oxide ions and hydrogen ions in the two electrodes can be written as:

$$\nabla(-K_i\nabla\phi_i) = Q \tag{7}$$

Where K_i denotes the ionic electrode conductivity (S m^{-1}), ϕ_i is the ionic potential (V) and Q is the current source term, as shown by Kim[9] can be defined according the Tafel equation as follows:

$$Q_{elc} = i_{o,elc}S_a\left\{\exp\left[\frac{0.5F(\phi_e - \phi_i - \Delta\phi_{e-elc})}{RT}\right] - \left(\frac{X_j}{X_{j-o}}\right)\exp\left[\frac{-0.5F(\phi_i - \phi_e)}{RT}\right]\right\} \tag{8}$$

Where $i_{o,elc}$ is the exchange current density for reaction (A m^{-2}) in electrodes (cathode or anode), X_j is the actual concentration of oxygen (cathode) and hydrogen (anode) respectively and X_{j-o} is reference concentration of oxygen in air and hydrogen in fuel, ϕ_e and ϕ_i are the electronic potential and ionic potential (V) respectively, S_a is specific surface area (m^2 m^{-3}).

The consumption term can be calculated as follows:

$$R_{i,cat} = \frac{Q_{cat}M_{O_2}}{4F} \quad \text{(Oxygen reduction)} \tag{9}$$

$$R_{i,an} = \frac{Q_{an}M_{H_2}}{2F} \quad \text{(Hydrogen oxidation)} \tag{10}$$

$$R_{i,an} = \frac{Q_{an}M_{H_2O}}{2F} \quad \text{(Water formation)} \tag{11}$$

The exchange current density for the reaction can be computed as follows:

$$i_{o,cat} = \gamma_{cat}\left(\frac{P_{O_2}}{P_{atm}}\right)^{0.25}\exp\left[\frac{-E_{act,cat}}{R_gT}\right] \quad (12)$$

$$i_{o,an} = \gamma_{an}\left(\frac{P_{H_2}}{P_{atm}}\right)\left(\frac{P_{H_2O}}{P_{atm}}\right)^{m}\exp\left[\frac{-E_{act,cat}}{R_gT}\right] \quad (13)$$

Equation [12],[13] were used in several papers; the values used for the above parameters varied and are summarized in Table 1 below:

In the electrolyte the reaction term Q is eliminated and then equation [7] becomes as follows:

$$\nabla(-K_i\nabla\phi_i) = 0 \quad (14)$$

Where the ionic conductivity K_i (S m^{-1}) can be calculated as described by Ferguson[4] as follows:

$$K_i = 6\times10^4\exp\left(\frac{-10300}{T}\right) \quad (15)$$

The electronic conduction at the two electrodes is defined as follows:

$$\nabla(-K_{e,cat}\nabla\phi_e) = -Q_{cat} \quad (16)$$

$$\nabla(-K_{e,an}\nabla\phi_e) = -Q_{an} \quad (17)$$

Where the electronic conductivities of the two electrodes can be calculated as follows:

For the anode two equations could be used, where the formulas dependent on the cell temperature as follows:

$$K_{e,an} = 3.35\times10^4\exp\left(\frac{-1392}{T}\right) \quad (18)$$

$$K_{e,an} = \frac{9.5\times10^7}{T}\exp\left(\frac{-1150}{T}\right) \quad (19)$$

The equation [18] for anode conductivity was used by P. Li[1], Bessette[13], and Massardo[14], while Ferguson[4] used formula of equation [19].

For the cathode three different equations were used in the literatures to calculate the cathode conductivity, equation [20] was used by P. Li[1] and equation [21] was used by Campanari[10], Bessette[13], Massardo[14] and Costamagna[15], while Ferguson[4] used formula of equation [22].

$$K_{e,cat} = 1.23\times10^4\exp\left(\frac{-500}{T}\right) \quad (20)$$

$$K_{e,cat} = 1.23\times10^4\exp\left(\frac{-600}{T}\right) \quad (21)$$

$$K_{e,cat} = \frac{4.2\times10^7}{T}\exp\left(\frac{-1150}{T}\right) \quad (22)$$

The momentum equation for flow in porous media, Darcy's law will be used, which states that the velocity vector is determined by the pressure gradient, the fluid viscosity and the structure of the porous media as follows:

$$\bar{u} = -\frac{K_p}{\mu}\nabla P \quad (23)$$

Where K_p denotes the permeability of the porous media (m^2), μ is the fluid viscosity (kg m^{-1} s^{-1}), P is the pressure (Pa), and $\bar{u}$ is the velocity vector (m s^{-1}).

The Darcy's law application mode combines with continuity equation as follows:

$$\frac{\partial\rho}{\partial t} + \nabla\cdot\rho\bar{u} = 0 \quad (24)$$

And substitute $\bar{u}$ from equation [23] in equation [24] we have the following:

$$\frac{\partial\rho}{\partial t} + \nabla\cdot\rho\left(-\frac{K_p}{\mu}\nabla P\right) = 0 \quad (25)$$

And by using equation of state or ideal gases $\left(\rho=\frac{PM_i}{R_gT}\right)$ and at the steady state we have the following:

$$\nabla\cdot\left(-\frac{K_pM_i}{\mu R_gT}P\nabla P\right) = 0 \quad (26)$$

The permeability (K_p) of the porous media can be calculated as shown by Jin Hyun Nam[16] as follows:

$$K_p = \frac{\varepsilon^3}{K_k(1-\varepsilon)^2(3\times10^5)^2} \quad (27)$$

Where K_k constant value is 5, for our case the porosity of anode (0.4), the permeability K_p value is 3.95e-13 m^2.

2.1 Boundary Conditions

Both of Dirchlit and Neumann boundary conditions at different physics mode will be used in this study as following:

2.2 Darcy's law boundary conditions

$P = P_o$ Pressure conditions (28)

$-\frac{K_p}{\mu}\nabla P\cdot n = 0$ An impervious or symmetric boundary condition (29)

Table 1. Parameters used in equations [12],[13]

γ_{cat} (Am^{-2})	γ_{an} (Am^{-2})	$E_{act,cat}$ (KJmole^{-1})	$E_{act,an}$ (KJmole^{-1})	m	Reference
7.0e9	7.0e9	120	110	1.0	[10]
7.0e8, 7.0e9	5.7e7,2.9e8,5.5e10	160,120	140,120	0.5,1.0	[11]
7.0e8	5.5e8	120	100	1.0	[12]

$-\frac{K_p}{\mu}\nabla P \cdot n = u_o$ Specific flow perpendicular to the boundary (30)

2.3 Maxwell-Stefan equation boundary conditions

$\omega = \omega_o$ For given mass fraction (31)

$$-n \cdot \left[\rho\omega_k\bar{u} - \rho\omega_k \sum_{l=1}^{n} \tilde{D}_{kl}\left(\nabla x_l + (x_l - \omega_l)\frac{\nabla P}{P}\right) + D^T\frac{\nabla T}{T}\right] = R_i$$

For given flux (32)

$$-n \cdot \left[\rho\omega_k\bar{u} - \rho\omega_k \sum_{l=1}^{n} \tilde{D}_{kl}\left(\nabla x_l + (x_l - \omega_l)\frac{\nabla P}{P}\right) + D^T\frac{\nabla T}{T}\right] = 0$$

For insulation/symmetry (33)

2.4 Conductive media DC application boundary conditions

$-n \cdot J = J_n$ For inward current flow (34)

$-n \cdot J = 0$ For electric insulation/no current across the boundary (35)

$V = V_o$ For electric-potential (36)

The above boundary condition specifies that the normal components of electric current are continuous across the interior boundary.

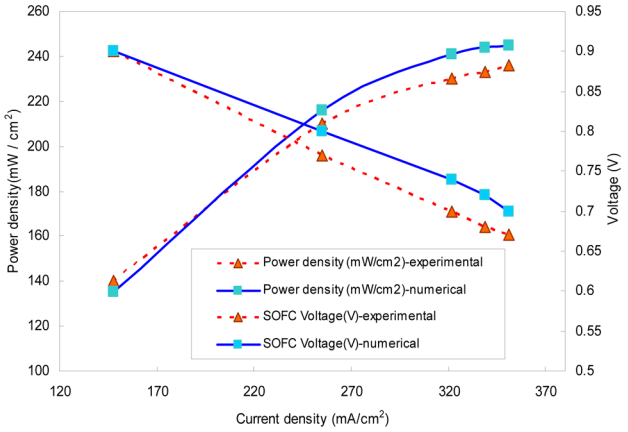

Fig. 2. Comparison of calculated and measured cell voltage of anode-supported tube SOFC versus cell current density.

3. Results and Discussion

Fig. 2 demonstrates the comparison of detailed-CFD calculations and an experimental data (voltage) and cell power density of an anode-supported tube SOFC at 750°C operating temperature done at Korean Institute of Energy Research (KIER). The fuel composition is 97% H_2, 3% H_2O and air is used as oxidant. As shown in Fig. 2 good agreement between the calculated results compared with the measured results for the cell voltage and cell power density is obtained.

Fig. 3 shows a two-dimensional cross section model for a

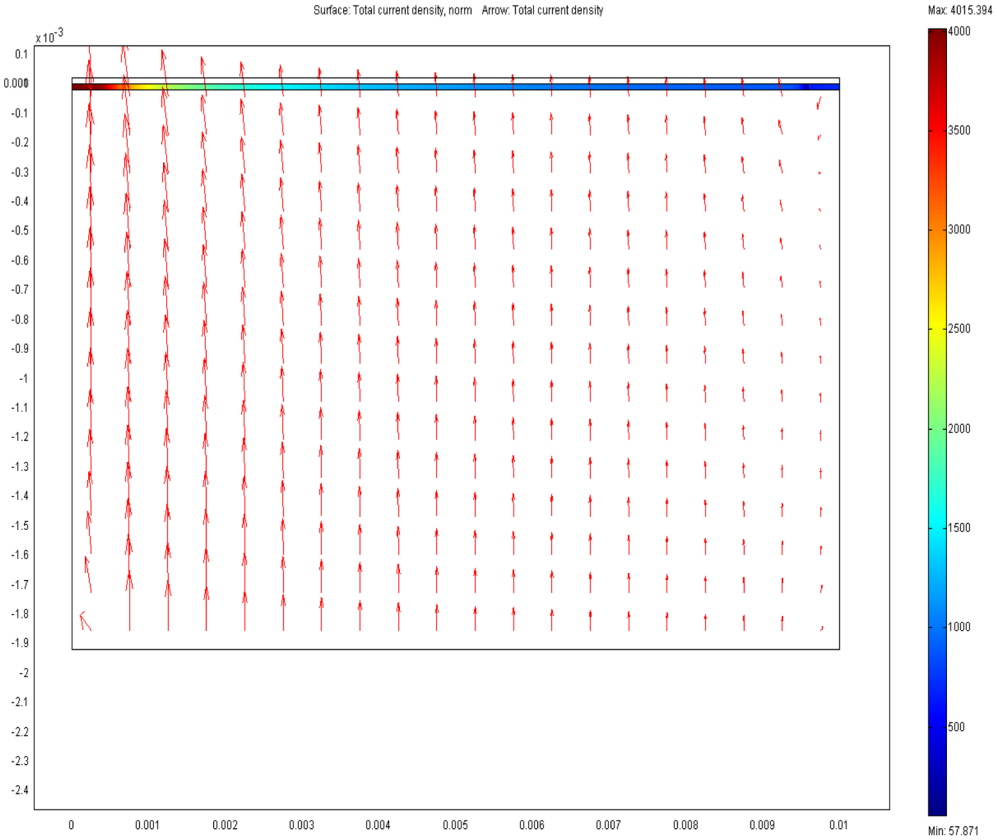

Fig. 3. Current density distribution in a SOFC-Anode supported tube at voltage difference between the two current collectors 0.65 V.

unit cell of anode-supported tube SOFC with a relatively high electronic conductivity. It is known that the current density distribution is one of the important design issues in fuel cells. As observed from the graph the current density is greater at the air inlet, where the oxygen concentration is the highest, and therefore provides better oxygen transport, while at he end, the current density is smaller because the fuel concentration is decreases.

Fig. 4 illustrates the weight fraction distribution of hydrogen in the anode at different current collectors' potentials 0.45 and 0.75 V. As shown at both potentials the higher hydrogen weight fraction value is obtained at lower left boundary (gas inlet) while the lower value is found at higher right corner of the anode. It is observed that the difference

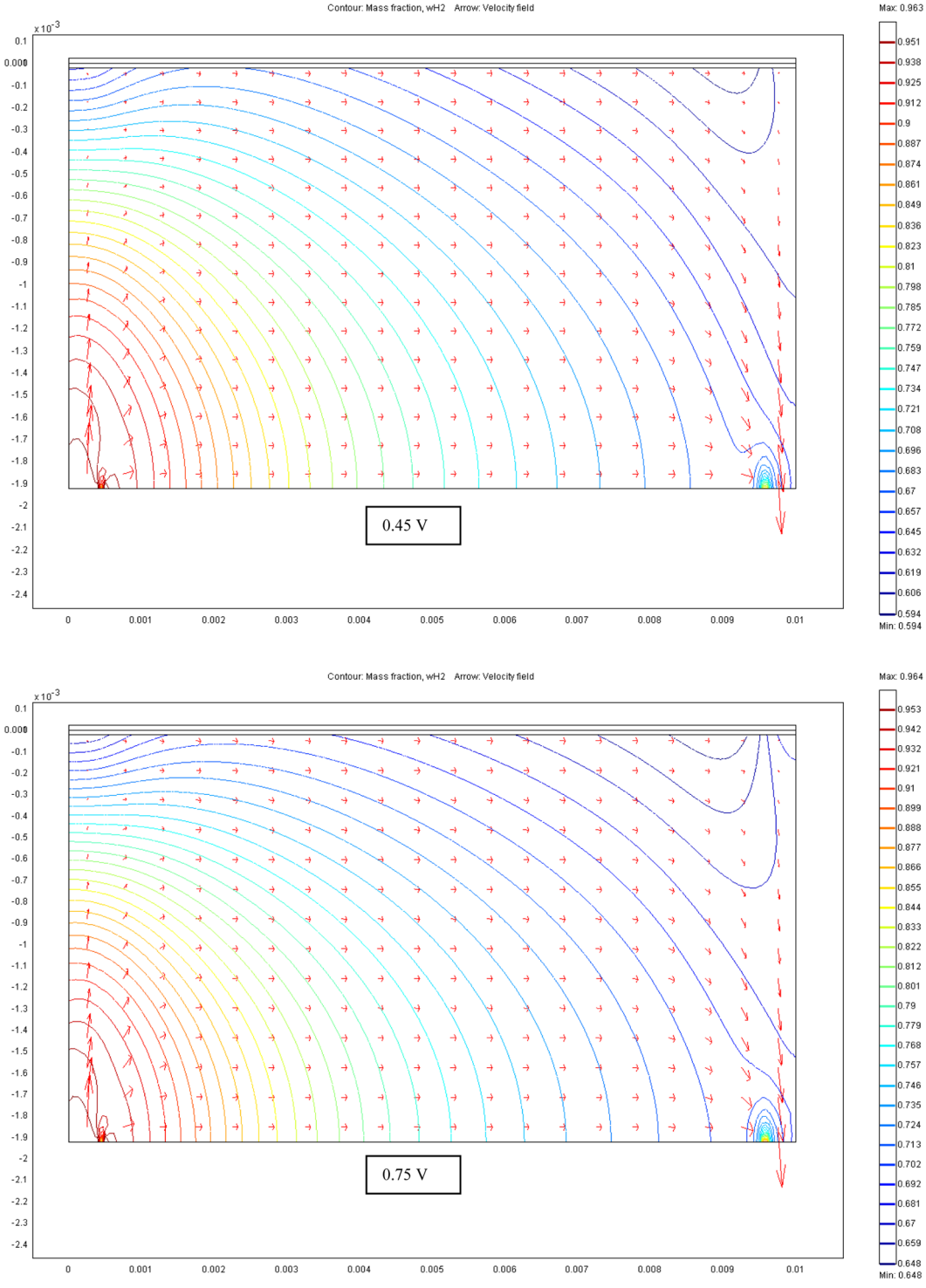

Fig. 4. Weight fraction distribution of Hydrogen in the anode at 0.45 and 0.75 cell potentials.

between maximum weight fraction consumption of hydrogen at cell voltage 0.45 V is about 38%, while at cell voltage 0.75 V is about 32%.

Fig. 5 demonstrates the weight fraction distribution of water produced in the anode at different current collector's potentials 0.45 and 0.75 V. As shown the lower cell potentials is higher current density consequently higher hydrogen consumption and higher water production.

4. Conclusions

Two-dimensional detailed-CFD cross section model for a unit cell of anode-supported tube SOFC has been developed to study the cell performance. Comparison between detailed-CFD

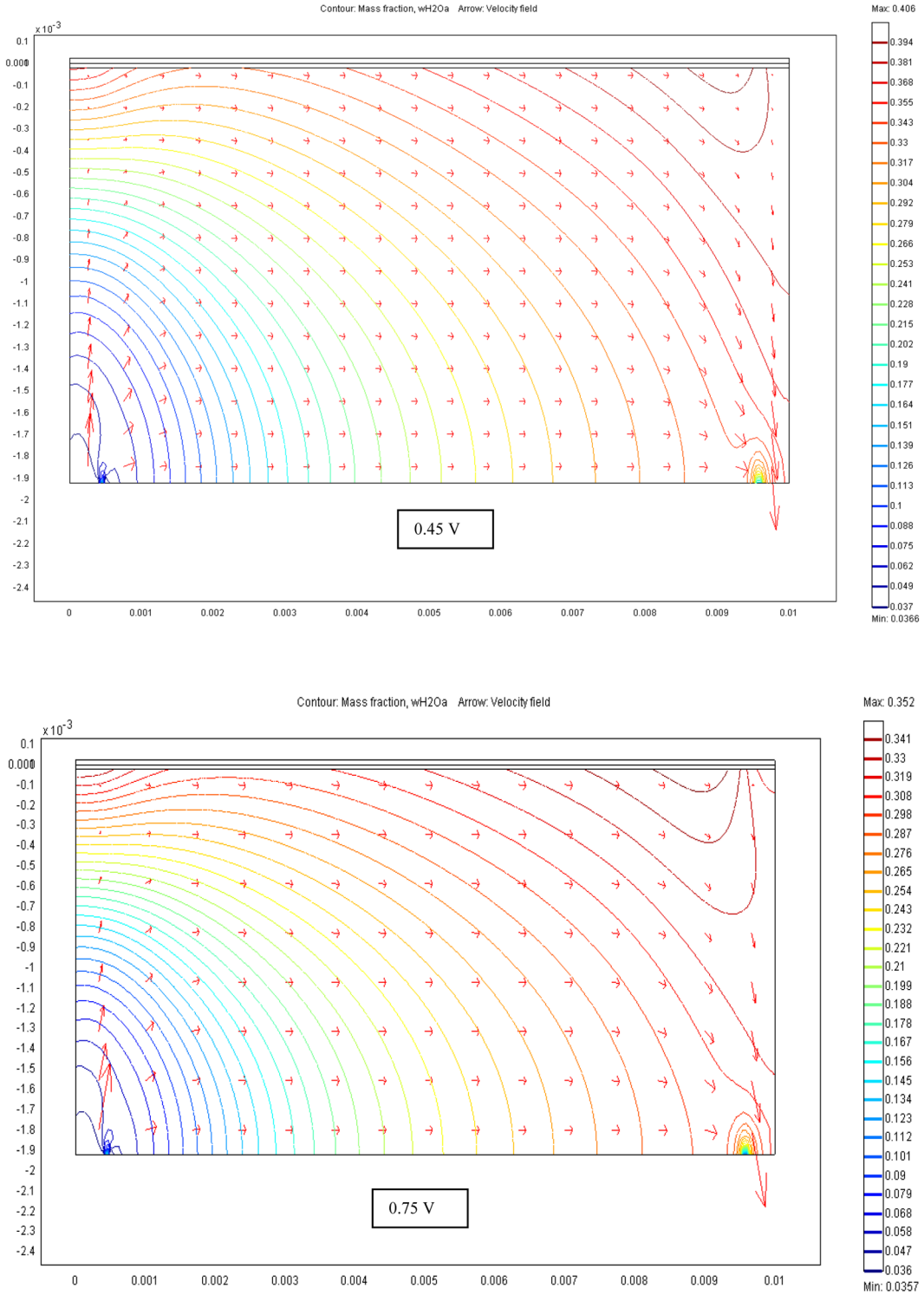

Fig. 5. Weight fraction distribution of water in the anode at 0.45 and 0.75 cell potentials.

calculations and an experimental data showed remarkable agreement for a polarization curves and cell power density versus cell current density. Dimensions and properties of the cell components are strongly affect on the performance of SOFC, so this type of modeling can help designers and developers to overcome certain limitations through simple design changes. In addition to current and potential distributions, the temperature distribution is also an important way to predict cell components material integrity and corrosion. For future work, energy equation (temperature parameter) will be added to the two- or the three-dimensional models to obtain a more complete picture of unit cell's performance and operating characteristics.

References

1. P.-W. Li and, M. K. Chyu, "Simulation of the Chemical/ Electrochemical reactions and heat/mass transfer for a tubular SOFC in a stack", *J. of Power Sources*, **124**, 487-498 (2003).
2. Y. X. Lu, L. Schaefer, and P. Li,"Numerical study of a flat-tube high power density solid oxide fuel cell: part I: Heat/mass transfer and fluid flow", *J. of Power Sources*, **140**, 331-339 (2005).
3. Y. X. Lu, and L. Schaefer, ,"Numerical study of a flat-tube high power density solid oxide fuel cell: part II : cell performance and stack optimization", *J. of Power Sources*, **153**, 68-75 (2006).
4. J. R. Ferguson, J. M. Fiard, and R. Herbin "Three-dimensional numerical simulation for various geometries of solid oxide fuel cells", *J. of Power Sources*, **58**, 109-122 (1996).
5. David J. Hall and R. Gerald Colclaser "Transient modeling and simulation of a tubular solid oxide fuel cell" IEEE Transactions on Energy Conversion, **14**(3), September (1999).
6. Roberto Bove, Piero Lunghi, and Nigel M. Sammes, "SOFC mathematic model for system simulations part one: from micro-detailed to macro-black box model", Int. *J. of Hydrogen Energy*, **30**, 181-187 (2005).
7. J. A. Wesselingh and R. Krishna, "Mass Transfer in Multi Component Mixture", Delft University Press (2000).
8. R. H. Perry, D. W. Green, and J. O. Maloney, Perry's Chemical engineers handbook, 7th ed., McGraw-Hill, New York (1997).
9. J. Kim, A. Virkar, K. Fung, K. Metha, and S. Singhal, "Polari-zation effects in intermediate temperature anode-supported solid oxide fuel cells" *J. Electrochemistry. Soc*., **146**, January (1999).
10. S. Campanari and P. Iora "Definition and sensitivity analysis of a finite volume SOFC model for a tubular Cell geometry", *J. of Power Sources*, **132**, 113-126 (2004).
11. P. Costamagna and K. Honegger "Modeling of Solid Oxide Heat Exchanger Integrated Stacks and Simulation at High Fuel Utilization" *J. Electrochemistry Soc*., **145 11**, 3995-4007 (1998).
12. P. Costamagna, A. Selimovic, M. D. Borghi, and G. Agnew. "Electrochemical model of the integrated Planar Solid Oxide Fuel Cell (IP-SOFC)" *Chemical Engineering Journal*, **102**, 61-69 (2004).
13. N. F. Bessette, W. J. Wepfer, and J. Winnick "A Mathematical Model of a Solid Oxide Fuel Cell" *J. of the Electrochemical Society*, **142**(11), 3792-3800 (1995).
14. A. F. Massardo and F. Lubelli "Internal Reforming Solid Oxide Fuel Cell – Gas Turbine Combined Cycles (IR SOFC-GT): Part A-Cell Model and Cycle Thermodynamic Analysis" *J. of Engineering for Gas Turbine and Power*, **122**, 27-35 (2000).
15. P. Costamagna, L. Magistri, and A. F. Massardo. "Design and part-load performance of a hybrid system based on a solid oxide fuel cell reactor and a micro gas turbine" *J. of Power Sources*, 96, 352-368 (2001).
16. J. H. Nam and D. H. Jeon "A Comprehensive micro-scale model for transport and reaction in intermediate temperature solid oxide fuel cells" *Electrochimica Acta*, **51**, 3446-3460 (2006).